Journal of Physics: Conference Series **585** (2015) 012005 doi:10.1088/1742-6596/585/1/012005

Hysteresis in column systems

P Ivanyi and A Ivanyi
Pollack Mihaly Faculty of Engineering and Information Technology, University of Pecs H-7624 Hungary

E-mail: peteri@morpheus.pte.hu

Abstract. In this paper one column of a telescopic construction of a bell tower is investigated. The hinges at the support of the column and at the connecting joint between the upper and lower columns are modelled with rotational springs. The characteristics of the springs are assumed to be non-linear and the hysteresis property of them is represented with the Preisach hysteresis model. The mass of the columns and the bell with the fly are concentrated to the top of the column. The tolling process is simulated with a cycling load. The elements of the column are considered completely rigid. The time iteration of the non-linear equations of the motion is evaluated by the Crank-Nicolson schema and the implemented non-linear hysteresis is handled by the fix-point technique. The numerical simulation of the dynamic system is carried out under different combination of soft, medium and hard hysteresis properties of hinges.

1. Introduction

Several engineering problems deal with the modelling of the non-linear behaviour of systems. The non-linear property of the engineering structures can be handled by single-valued or two-valued hysteretic characteristics. Generally two questions arise here, how to model the non-linear, hysteretic characteristics of the structure and how to insert this model into the simulation method of the system.

The non-linearity of thermal, magnetic and mechanical systems can be realized with microscopic, mesoscopic and macroscopic simulations. The simplest representation of non-linear characteristics is the macroscopic model, where the purpose is the phenomenological description of the physical process. On the other hand a more detailed approach to describe the non-linear behaviour of the structure or material is the microscopic model, where the elementary scale of the material is simulated from the energetic point of view. The non-linearity of material domains/clusters can be analysed by the Stoner-Wohlfarth type [1] and the Jiles-Atherton type models [2]. The mesoscopic description of the hysteresis behaviour with respect to some physical properties can be found in the Preisach type models [3]-[10], which is the most popular modelling of non-linearity of materials and structures.

The above-summarized general trend can also be found in the simulation of non-linear behaviour of mechanical systems.

To handle the non-linearity of joints in steel frames different phenomenological models have been developed. The range of these models varies from the so-called empirical models through the analytical simulations [11], [12] to the very popular different level of the Ramberg-Osgood and the Richard-Abbott models [13]-[19]. To build up the material from elementary clusters and modelling their mechanical behaviour is developed in microscopic models in Reference [20]. To represent the hysteresis of steel due to the stress and strain effects the modified versions of Jiles-Athertom models can be used [21], [22] and in the modified models with loss separation under different stresses [23].

There is a continued research to extend the Preisach model for the simulation of mechanical properties of materials and to describe the non-linear behaviour of steel structures [24]-[26].

The purpose of the recent research is to extend the Preisach model for the theoretical investigation of semi-rigid joints of hinges in a two storey steel column structure and insert the model into the computation of the column systems.

2. The bell tower

In Pécs, city of Hungary, there is a Turkish style mosque on the main square of the city centre, which functions as a Christian church nowadays. Pécs was the Cultural Capital of Europe in 2010. During the preparation period of this event a bell tower has been designed to the northeast corner of the mosque with the statue of St. Bartholomew (figure 1) by two architects: Zoltan Bachman and Balint Bachmann [27]. The three bells are surrounded by three slender steel columns. The bell tower has a moving telescopic structure, which can hydraulically rise to become a tower (figure 2). The designed form of the bell tower can be seen in figure 3.

Considering the structure of the bell tower, two sensitive points should be investigated during the tolling action, the fixed support at the bottom and the joint between the lower and upper columns. To model the behaviour of this dynamic system, first, one column with semi rigid hinges of non-linear hysteretic characteristic is modelled. In this way it is possible to check how the hinges behave during the dynamic action.

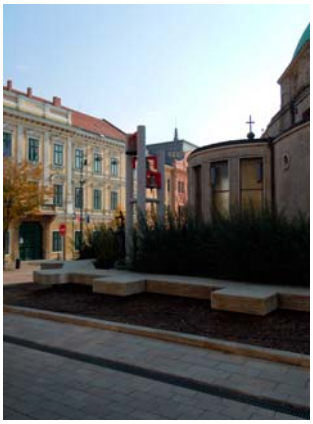

Figure 1. St Bartholomew's bell tower.

Figure 2. The telescopic height of the bell tower.

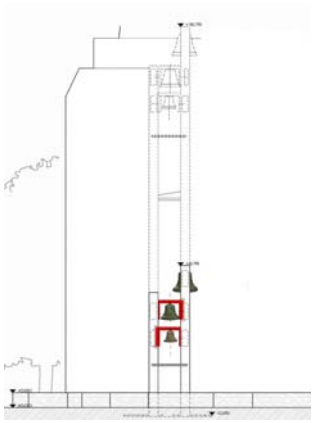

Figure 3. The designed form of the bell tower.

3. The model of the dynamic system

In this paper one column of the bell tower is modelled. It is built from two cylindrical shape tubes with the lower part of diameter $d_{1ex} = 0.3\,\mathrm{m}$ and the thickness is $8\,\mathrm{mm}$ ($d_{1in} = 0.284\,\mathrm{m}$). The upper part has diameters $d_{2ex} = 0.282\,\mathrm{m}$ and $d_{2in} = 0.266\,\mathrm{m}$. The length of the lower column is $l_1 = 5.35\,\mathrm{m}$, while the upper column is $l_2 = 8\,\mathrm{m}$ long. The masses m_1, m_2 of the columns are concentrated to the upper end of the columns. The mass of the bell (290 kg) and the fly (40 kg) (figure 4) is added to the mass of the upper column.

As a result of the cycling external force the columns have declinations angles φ_1, φ_2 around of the joint points, resulting in deflections u_1, u_2 (figure 5). Considering small declination $u \approx \varphi l$, ($\sin\varphi \approx \tan\varphi \approx \varphi$, $\cos\varphi \approx 1$) a bending moment from the external cycling force and from the mass of the columns arises.

To model the moment of the electrical motor for forcing the bells to toll, a concentrated, horizontal, exponentially increasing, periodically changing force is acting during the tolling process with the amplitude $F_0 = 1\,\mathrm{kN}$ (figure 6) and cycling periodicity $T_p = 0.2\,\mathrm{s}$,

$$F(t) = F_0\left(1 - e^{-t/T_p}\right)\sin\left(\frac{2\pi}{T_p}t\right). \tag{1}$$

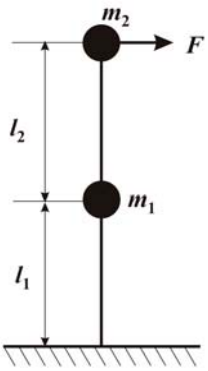

Figure 4. The column system.

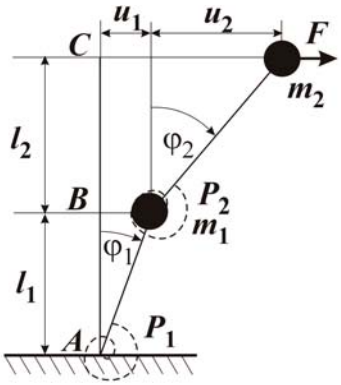

Figure 5. Deflection and declination of the columns.

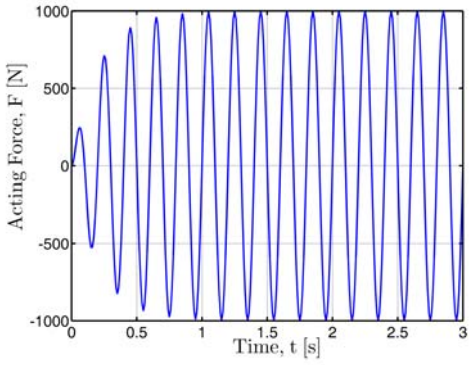

Figure 6. The cycling load of the columns.

The two parts of the column can be considered as a semi rigid cantilever. The bottom point of the lower column (point A) and the joining point between the two columns (point B) are modelled with rotational springs. The behaviour of the rotational springs is modelled with hysteresis characteristics between the spring moment (P) and the declination angle (φ), $\varphi = \mathcal{H}\{P\}$. During the investigations three types of characteristics are considered for the rotational springs as soft (H1), medium (H2) and hard (H3) as it can be seen in figure 7.

In mechanical systems the characteristics of spring moment-declination angle are used, however in this case the Preisach hysteresis model is introduced to describe the behaviour of the rotational springs, so the inverse hysteresis is constructed (figure 8).

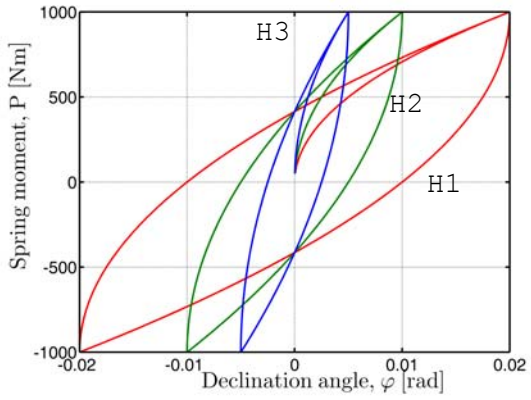

Figure 7. Direct characteristics of the rotational springs.

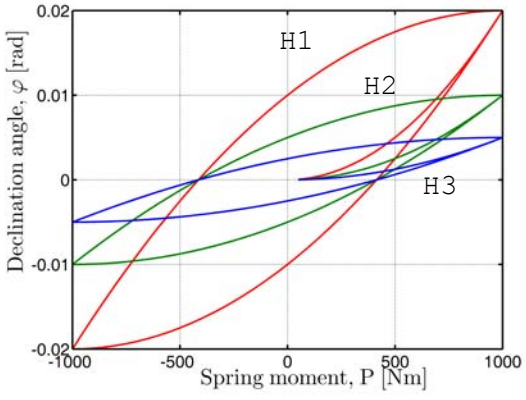

Figure 8. The Preisach model of hysteresis.

Introducing the elementary hysteron $\gamma(\alpha,\beta)$ of the Preisach model for handling the non-linear behaviour of the elementary cluster of the rotational spring, where α,β are the switching fields, the distribution function $\mu(\alpha,\beta)$ weights the effect of the elementary operator $\gamma(\alpha,\beta)$, while $P(t)$ is the

acting spring moment [28]. The declination angle as the output of the non-linear spring can be determined as

$$\varphi(t,P)=\iint\limits_{\alpha\geq\beta}\mu(\alpha,\beta)\gamma(\alpha,\beta)P(t)\,d\alpha\,d\beta\,. \tag{2}$$

The integration is evaluated over the Preisach triangle, defined as $\alpha\geq b$, while $\alpha\in[-1,\cdots,1]$, $\beta=[-1,\cdots,1]$.

4. Formulation of the dynamic motion

The elements of the steel columns are considered to be completely rigid. To describe the dynamic behaviour of the above system, the relation between the bending moment and the declination has to be determined. As the system plotted in figure 4 has two bars with two hinges at points (A) and (B), the motion will be determined by the bending moment acting at these points [29], [30]. The system damping effect is represented with the hysteresis loss.

The acting bending moment originating from the external force and the mass positioned to the top end of the columns accelerates the rotation and acts on the rotational spring at point (A) as

$$I_{2A}\ddot{\varphi}_2+I_{1A}\ddot{\varphi}_1+P_1=F(l_1+l_2)+G_2(u_1+u_2)+G_1u_1, \tag{3}$$

where I_{1A} and I_{2A} are the inertia moments of mass m_1 and m_2 at point A,

$$I_{1A}=m_1l_1^2,\quad I_{2A}=m_2(l_1+l_2)^2, \tag{4}$$

P_1 is the bending moment action on the rotational spring at point (A) and G_1,G_2 are the gravity forces of m_1,m_2.

At point B the upper column acts and the acceleration of rotation can be formulated as

$$I_{2b}\ddot{\varphi}_2+P_2=Fl_2+G_2u_2, \tag{5}$$

where I_{2B} is the inertia moment of mass m_2 at point B,

$$I_{2B}=m_2l_2^2\,. \tag{6}$$

Taking into account the condition of small declination and representing the deflections as

$$u_1=\varphi_1l_1,\quad u_2=\varphi_2l_2\,, \tag{7}$$

the second order non-linear differential equations have the form of:

$$\begin{aligned}&I_{2A}\ddot{\varphi}_2+I_{1A}\ddot{\varphi}_1+P_1=F(l_1+l_2)+G_2[\varphi_1l_1+\varphi_2l_2]+G_1\varphi_1l_1,\\&I_{2b}\ddot{\varphi}_2+P_2=Fl_2+G_2\varphi_2l_2,\end{aligned} \tag{8}$$

$$\varphi_1=\mathcal{H}\{P_1\},\quad \varphi_2=\mathcal{H}\{P_2\}. \tag{9}$$

5. Numerical iteration

An analytical solution of the above dynamic problem can be determined as it is proved in [31]. For the numerical approximation of the dynamic problem (8), (9) the time discretisation is evaluated by the double application of the Crank-Nicolson schema [32]. The non-linear iteration is realized by the fix-point technique [33], [34] to have a contract transformation of the direct characteristics

$$P(\varphi)=k_{FP}\varphi+R\,, \tag{10}$$

where k_{FP} is the fix-point constant to represent the linear part of the connection stiffness, $k_{FP}\varphi$ and R is the residual non-linearity. Substituting (10) into (8) at a fixed time moment, n,

$$\begin{aligned} I_{2A}\ddot{\varphi}_{2n}^{i+1} + I_{1A}\ddot{\varphi}_{1n}^{i+1} + k_{AFP}\varphi_{1n}^{i+1} &= M_{An}^{i} - R_{An}^{i}, \\ I_{2b}\ddot{\varphi}_{2n}^{i+1} + k_{BFP}\varphi_{2n}^{i+1} &= M_{Bn}^{i} - R_{Bn}^{i}, \end{aligned} \tag{11}$$

where M_{An}^{i} and M_{Bn}^{i} are the bending moments at points (A) and (B), at time moment n of iteration step i

$$\begin{aligned} M_{An}^{i} &= F_n(l_1 + l_2) + G_2\left(\varphi_{1n}^{i} l_1 + \varphi_{2n}^{i} l_2\right) + G_1\varphi_{1n}^{i} l_1, \\ M_{Bn}^{i} &= F_n l_2 + G_2\varphi_{2n}^{i} l_2. \end{aligned} \tag{12}$$

The iteration steps are as follows:

Step 1, At the new $n-$th time step the initial value of the declination angle is equal to the last value of the previous time step, $\varphi_n^i = \varphi_{n-1}$. The initial value of the non-linear part of the hysteresis is equal to the last value of the previous time step, $R_n^i = R_{n-1}$;

Step 2, The value of the acting bending moments are known from (12) with respect to the iteration of declination φ_n^i;

Step 3, With the solution of (11) a new iteration for the declination φ_n^{i+1} can be determined;

Step 4, An estimation for the bending moment acting on the rotational spring can be determined as $P_n^{i+1} \approx k_{FP}\varphi_n^{i+1} + R_n^i$;

Step 5, With the hysteresis (9) the remaining non-linear part can be calculated as $R_n^{i+1} = P_n^{i+1} - k_{FP} \cdot \mathcal{H}\left\{P_n^{i+1}\right\}$;

Step 6, The iteration continues on while $\left\|R_n^{i+1} - R_n^i\right\| > \varepsilon\left\|R_n^{i+1}\right\|$, otherwise $x_n^i = x_n^{i+1}$, $R_n^i = R_n^{i+1}$ and go to Step 2.

6. Simulation results

The numerical realization of the above theory has been developed in MATLAB code and the hysteresis has been introduced to the numerical iteration.

In all cases the time interval of the investigation is 3 s. The cycling time was selected as 0.2 s, in one period 20 time steps have been investigated, so the time discretisation was 0.01 s.

According to the different techniques to connect the elements of the telescopic construction and to fix the support of the bottom column, different properties of the rotational springs at points (A) and (B) have been considered. In table 1 the properties of the investigated rotational spring configurations are listed.

Table 1. Rotational springs at the nodes

Case	1	2	3	4	5
Point A	H2	H2	H1	H1	H2
Point B	H2	H3	H2	H3	H1

Case 1: First, it is assumed that both of the rotational springs have the same non-linearity, the hysteresis characteristics are assumed to be medium type (H2) at points (A) and (B).

At point (A) the variation of the declination angle versus the spring moment can be seen in figure 9, while at point (B) the hysteresis of the rotational spring generated between the declination angle and the spring moment is plotted in figure 10.

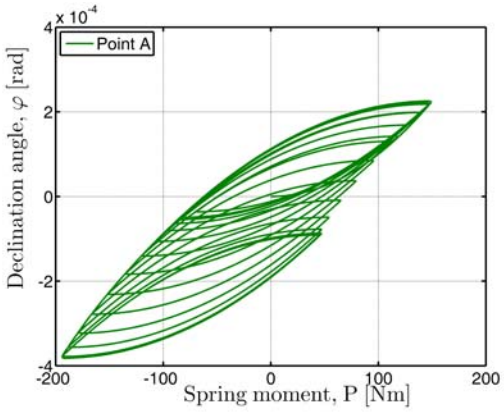

Figure 9. The hysteresis of the rotational spring at point (A).

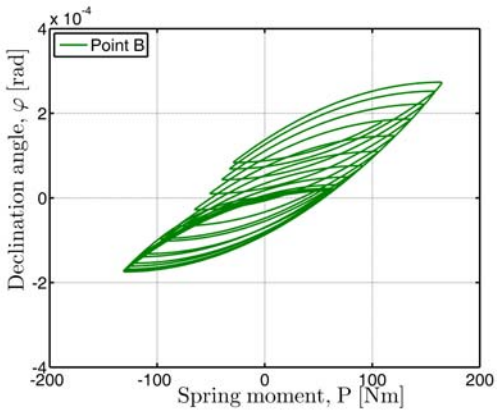

Figure 10. The hysteresis of the rotational spring at point (B).

From the figures it can be seen, that although both of the rotational spring has the same property, according to the different loads and positions, the two springs have different hysteresis. At the bottom point (A) of the lower column the rotation of the spring is more intensive compared to the spring at the joint between the upper and lower columns, point (B).

Similar properties are shown by the deflections of the end points of columns at points (B) and (C). According to the acting force the end points of the columns have deflection u_1 at the joint of the columns (B) and u_2 at the top point of the upper column (C), as it can be seen in figure 11 and figure 12.

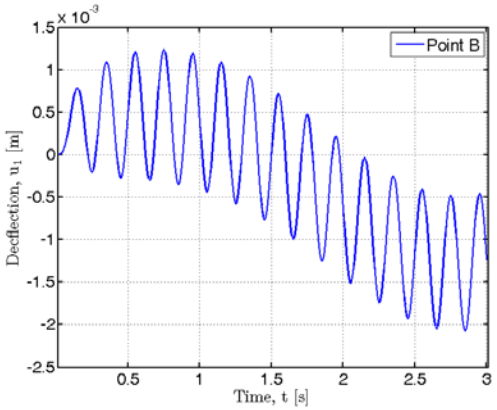

Figure 11. Deflection at point (B).

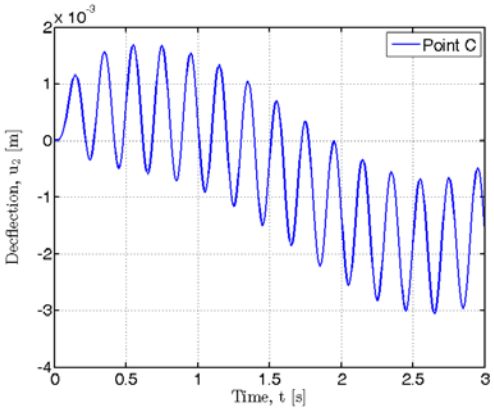

Figure 12. Deflection at point (C).

The deflection at the end point of the structure is more intensive; within the 3 s tolling period the maximum value of deflection at the free end of the structure is about 3 mm, while the maximum deflection at the joint point between the upper and lower columns is about 2 mm.

Case 2: In the next case the rotational spring at the fixed point of the bottom column, point (A), remains the same as before, medium style (H2), while at the joint point between the upper and lower columns, point (B), the rotational spring has hard properties (H3). Loading the system with the same external force and evaluating the simulation under the same time steps, the rotational hysteresis at the bottom point (A) is plotted in figure 13, while the rotational hysteresis of the spring at point (B) is plotted in figure 14.

From the figures it can be seen, that if the joint point between the upper and lower columns is fixed harder than the bottom point of the column, the declination angles at both points (A) and (B) are decreasing.

Considering the deflections of point (B) and at the free end of the column system, point (C), at both places the deflections are decreasing as well, as it can be seen in figure 15 and figure 16. The maximum deflection at point (B) is about 1.2 mm, while at the free end of the column (C) this deflection is about 1.6 mm.

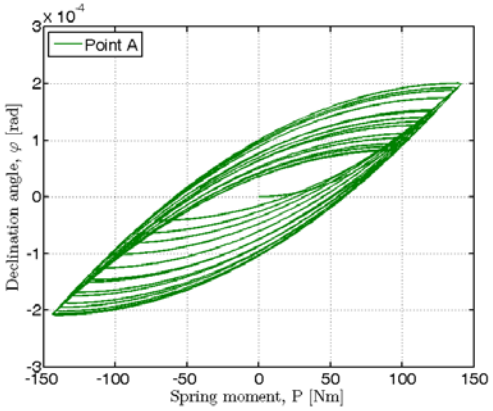

Figure 13. The rotational spring of medium property at point (A).

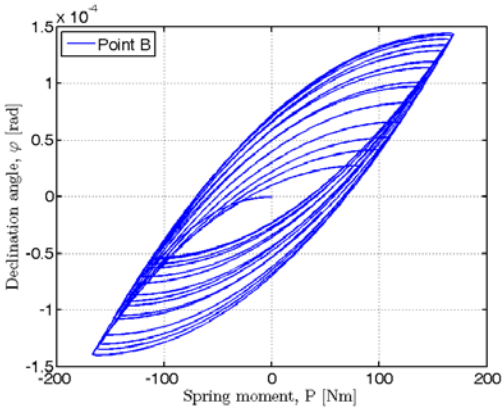

Figure 14. The rotational spring of hard property at point (B).

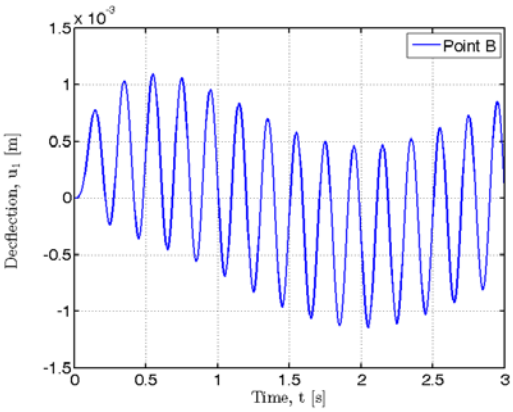

Figure 15. Deflection at the middle point of the column, at point (B).

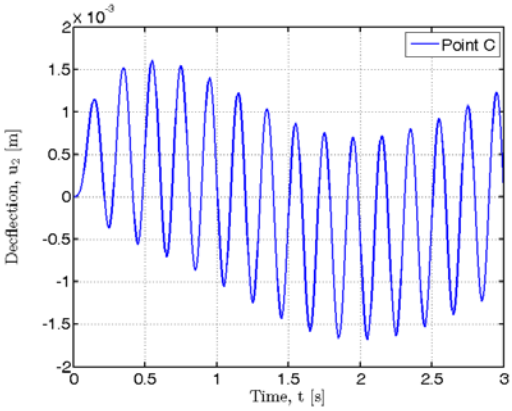

Figure 16. Deflection at the free end of the column, at point (C).

Case 3: Now the rotational spring at the fixed point of the bottom column, point (A), is selected to have weak property (H1), while at the joint point between the upper and lower columns, point (B), the rotational spring has medium property (H2).

For the cycling external force in this case during the motion of the column the hysteresis of the hinges became more stable as it can be seen in figure 17 and figure 18.

Similar stable cycling motion can be observed in the deflections at the joining point between the upper and lower columns, point (B), and at the free end of the column, point (C), as it is plotted in figure 19 and figure 20.

From the figures it can be seen, that however at the fixed point of the bottom column, point (A), the rotational spring has soft property (H1), and at the joint point between the upper and lower columns, point (B), the rotational spring has medium property (H2), the deflections became smaller. At point (B) its maximum value after the first peak is about 1.0 mm, while at point (C) the maximum value of the deflection is about 1.5 mm.

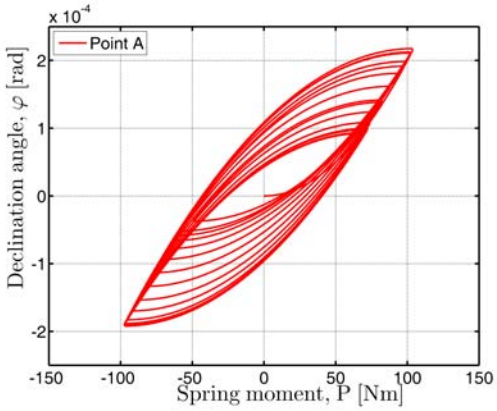

Figure 17. The rotational spring of soft property at point (A).

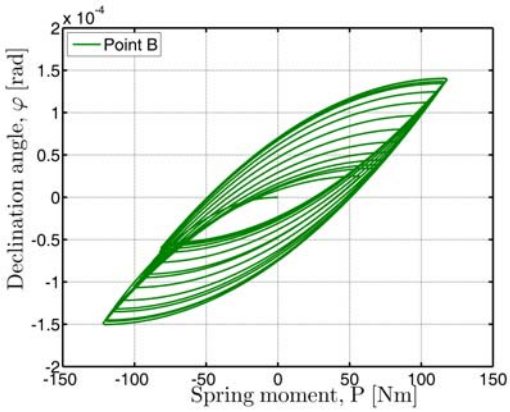

Figure 18. The rotational spring of medium property at point (B).

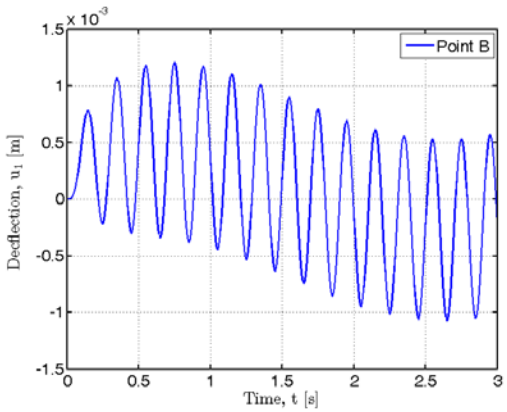

Figure 19. Deflection of the column at point (B).

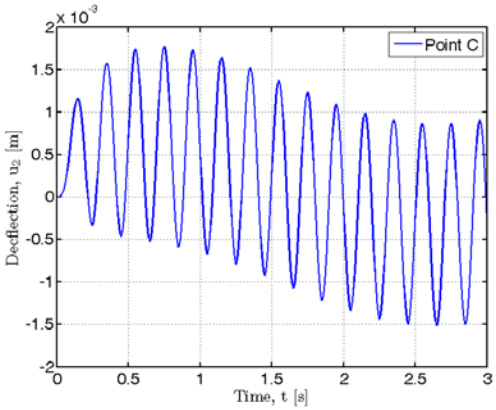

Figure 20. Deflection at the free end of the column, at point (C).

Case 4: The stabilization of the cycling motion can be observed if at the joint point between the upper and lower columns the property of the rotational spring is harder than the property of rotational spring at the fixed point of the bottom column. So, in this case the rotational spring at the fixed point of the lower column, point (A), remain soft (H1), while at the joint point between the upper and lower columns, point (B), the rotational spring is supposed to have hard property (H3).

The hysteresis curves of rotational springs seem to be stabilized during the tolling action as it can be seen at the rotational spring of point (A) in figure 21 and at the rotational spring of point (B) in figure 22.

The hysteresis curves contain some offset during the motion, which can be explained by the mass positioned at the end of each column. The bending moments generated by the gravity force has a constant load on the system and this is added to the cycling load and it results in the offset in the declination and deflection as well.

The deflection at the joint of the columns (point B) and at the free end of the upper column (point C) is plotted in figure 23 and figure 24.

From the figures it can be seen, that under cycling load, at the joining point between the upper and lower columns, point (B), the stabilization of the dynamic system results in the maximum deflection with amplitude about 1.1 mm and at the free point of the column, point (C), the maximum deflection is about 1.6 mm.

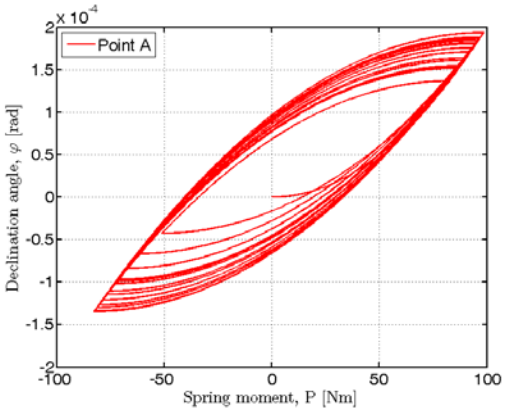

Figure 21. The declination of the soft rotational spring at point (A).

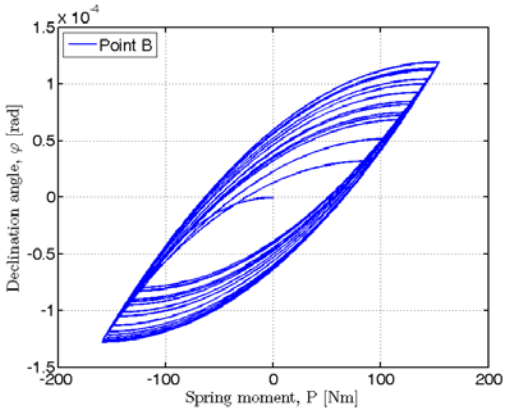

Figure 22. The declination of hard rotational spring at point (B).

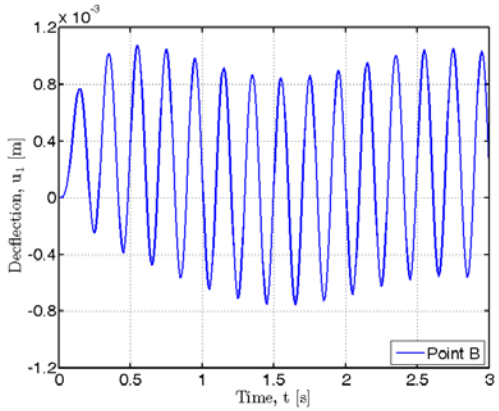

Figure 23. Deflection of the soft rotational spring at the joint point of the cantilevers, in point (B).

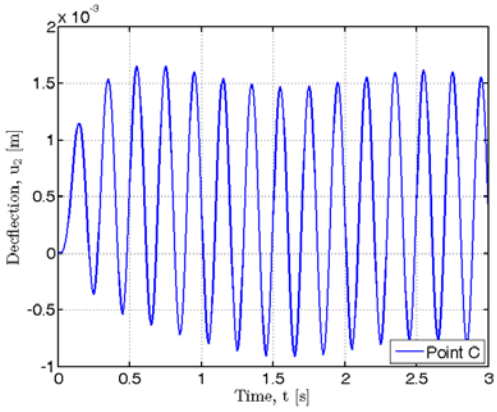

Figure 24. Deflection of the hard rotational spring at he free end of the column system, in point (C).

From the previous studies it can be seen that in all the cases if the rotational spring at the fixed point (A) of the bottom column is even softer than the rotational spring at the joint point between the upper and lower columns, point (B), during the dynamic process the system became stable, see figure 13–14, figure 17-18 and figure 21-22.

The hysteresis curve characterizing the declination of the rotational springs results in stable cycling motion with a small offset. In a similar way, the deflections at the joint of the columns (point B) and at the free end of the upper column (point C) prove to stabilize the elongation as it can be seen in figure 15-16, figure 19-20 and figure 23-24.

Case 5: In this case if the rotational spring at the fixed point of the bottom column (point A) has the same medium property (H2) as the rotational spring at the joining point between the upper and lower columns (point B), some tendency of instability can be observed as it is shown in figure 9-10.

Thus, in the next case the property of the rotational spring at the joining point of the columns (point B) is selected to be softer (H1) than at the fixed point of the bottom column (point A), where the rotational spring is selected to have medium property (H2).

After the numerical simulation at the fixed point of the bottom column (point A) as well as at the joint point of the columns the hysteresis curves definitely exhibit instability as it can be seen in figure 25 and figure 26. According to the soft property of the rotational spring at point B during the cycling load the offset of the hysteresis curves is increasing, finally the failure of the upper column will occur.

Similar instability can be observed in the deflection at the joint of the columns (point B) as well as at the free end of the upper column (point C) as it is plotted in figure 27 and figure 28.

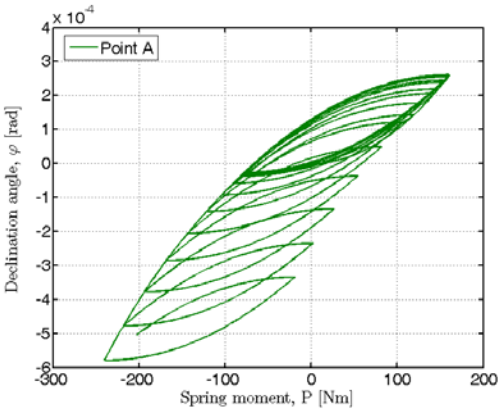

Figure 25. The declination of the medium property of rotational spring (H2) at the fixed point of the column (point A).

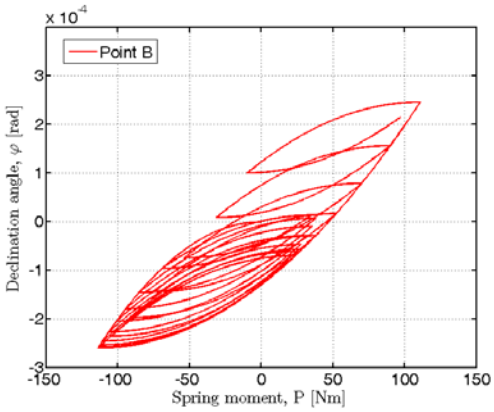

Figure 26. The declination of the soft property of the rotational spring (H1) at the joint point of the columns (point B).

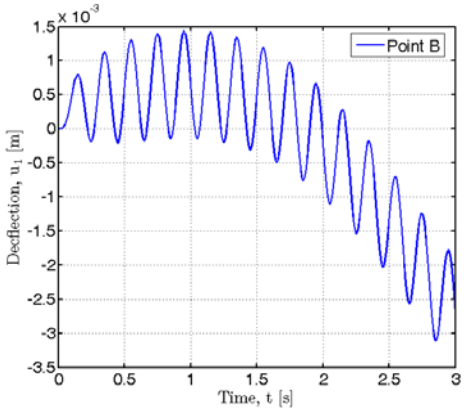

Figure 27. The deflection at the joint of the columns (point B).

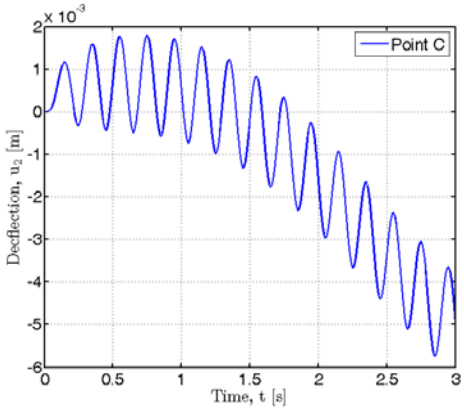

Figure 28. Deflection of the free end of the column (point C).

According to the telescopic construction of the column in this last case instability can be observed in the behaviour of the bell tower. The instability can be observed in the deflection of the whole system as it is shown in figure 29.

7. Conclusion

In this research one column of a telescopic construction of a bell tower has been investigated. The hinges at the fixed support of the bottom column and at the joint of the columns have been modelled with rotational springs of hysteresis characteristics. The mass of the columns and the bell with the fly are concentrated to the top of each column. The tolling process is modelled with a cycling load. The elements of the column are considered to be completely rigid. The non-linear equation of motion is solved by the double application of the Crank-Nicolson schema; the iteration on the non-linear hysteresis characteristic is evaluated by the fix-point technique.

Numerical simulations have been performed assuming the combination of different, soft, medium and hard hysteresis characteristics of hinges. The analytical results prove that in the case when at the fixed point of the bottom column the hinge has softer hysteresis characteristic than at the joint of the columns, the dynamic behaviour of the system can be stable. However, in the case when the hinge at

the joint of the columns is softer than the one at the fixed support of the bottom column, the instability of the system can be observed.

Figure 29. The instability property of the construction under cycling load.

8. References

[1] Stoner EC and Wohlfarth EP 1991 Reprinted in *IEEE Tr. on Magn*. **27** 3457
[2] Jiles DC and Atherton DL 1986 *J. of Magn. and Mag. Materials* **61** 48
[3] Chikazumi S and Charap SH 1964 *Physics of Magnetism* (J. Wiley)
[4] Krasnosel'skii MA and Pokrovskii AV 1983 *System with Hysteresis* (in Russian) (Moscow: Nauka)
[5] Mayergoyz ID 1991 *Mathematical Model of Hysteresis* (Springer)
[6] Visintin A 1994 *Differential Models of Hysteresis* (Springer)
[7] Brokatte M and Sprekels J 1996 *Hysteresis and Phase Transitions* (Springer)
[8] Ivanyi A 1997 *Hysteresis Models in Electromagnetic Computation* (Budapest: Akademiai Kiado)
[9] Bertotti G 1998 *Hysteresis in Magnetism, for Physicists, Material Scientists, and Engineers* (NY: Academic Press)
[10] Della Torre E 1999 *Magnetic Hysteresis* (NY: IEEE Press)
[11] Díaz C, Martí P, Victoria M and Querin OM 2011 *J. of Constructional and Steel Research* **67** 741
[12] Kwofie S 2003 *Material and Engineering* **A357** 86
[13] RambergW and Osgood WR 1943 Technical Note No. 902 *National Advisory Committee for Aeronautics* (Washington DC)
[14] Demartino A, Landolfo R and Mazzolani FM 1990 *Materials and Structures* **23** 59
[15] Skelton R P, Maier HJ and Christ HJ 1997 *Material Science in Engineering* **A238** 377
[16] Mostaghel N and Byrd RA 2002 *Int. J. of Non-Linear Mechanics* **37** 1319
[17] Niesłony A, el Dsoki C, Kaufmann H and Krug P 2008 *Int. J. of Fatigue* **30** 1967
[18] Ni YQ, Wang JY and Ko JM 1999 Advanced method for modelling hysteretic behaviour of semi-rigid joints *Proceedings of the Second Int. Conf. on Advances in Steel Structures* (Hong Kong, China, 15-17 December 1999) (in *Advances in Steel Structures*) ed SL Chan and JG Teng (Elsevier) vol 1 pp 331–338
[19] Richard MR and Abbott BJ 1975 *J. Eng. Mech. Div. ASCE* 1975 **101** 4 511
[20] Smith RC, Seelecke S, Dapino M and Ounaies Z 2006 *J. of the Mechanics and Physics in Solids* **54** 46
[21] Anglada-RiveraJ, Padovese LR and Capó-Sánchez J 2001 *J. of Magn. and Mag. Materials* **231** 299

[22] Steven KJ 2000 *NDT&E International* **33** 111
[23] Permiakov V, Dupré L, Pulnikov A and Melkebeek J 2004 *J. of Magn. and Mag. Materials* **272–276** e2553
[24] Aleshin V and Van Den Abeele K 2005 *J. of the Mechanics and Physics of Solids* **5553** 795
[25] Bolshakov GV and Lapokov AJ 1996 *J. of Magn. and Mag. Materials* **162** 112
[26] BerquistA and Engdahl G 1996 *IEEE Trans. on Magn*. **27** 112
[27] BachmannB and Bachman Z 2010 *Pollack Periodica* **5** 3 19
[28] Kuczmann M and Ivanyi A 2008 *The Finite Element Method in Magnetics* (Budapest: Akademiai Kiado)
[29] Chan SL and Chui PPT 2000 *Nonlinear Static and Cycling Analysis of Steel Frames with Semi-rigid Connections* (Elsevier)
[30] Maroti Gy 2011*Pollack Periodica* **6** 1 141
[31] Krejci P 1988 *Application of Mathematics* **33** 145
[32] Ivanyi A 2003 *Continuous and Discrete Simulations in Electrodynamics* (Budapest: Akademiai Kiado)
[33] Bottachio O, Chiampi M and Ragusa C 2003 *IEEE Trans. on Magn.* **34** 1179
[34] KuczmannM 2011 *Physica B* Condensed Matter **406** 1403